FORM TI-12
12/97

WAPD-T-3181

CONF-980708--

RESIDUAL STRESSES IN WELD DEPOSITED CLAD PRESSURE VESSELS AND NOZZLES

D. P. Jones and W. R. Mabe
Westinghouse Electric Company,
a Division of CBS Corporation
West Mifflin, PA 15122-0079

J. R. Shadley and E. F. Rybicki
University of Tulsa
Tulsa, Oklahoma 74104-3189

DE-AC11-93PN38195

BETTIS ATOMIC POWER LABORATORY   WEST MIFFLIN, PENNSYLVANIA 15122-0079

Operated for the U.S. Department of Energy
by WESTINGHOUSE ELECTRIC COMPANY,
a division of CBS Corporation

(This Page Intentionally Blank)

DISCLAIMER

Residual Stresses in Weld Deposited Clad Pressure Vessels and Nozzles

D. P. Jones & W. R. Mabe
Westinghouse Electric Company
A Division of CBS
West Mifflin, PA 15122-0079

J. R. Shadley & E. F. Rybicki
The University of Tulsa
Tulsa, OK 74104-3189

ABSTRACT

Results of through-thickness residual stress measurements are provided for a variety of samples of weld deposited 308/309L stainless steel and Alloy 600 cladding on low-alloy pressure vessel ferritic steels. Clad thicknesses between 5 and 9 mm on samples that vary in thickness from 45 to 200 mm were studied. The samples were taken from flat plates, from a spherical head of a pressure vessel, from a ring-segment of a nozzle bore, and from the transition radius between a nozzle and a pressure vessel shell. A layer removal method was used to measure the residual stresses. The effects of uncertainties in elastic constants (Young's modulus and Poisson's ratio) as well as experimental error are assessed. All measurements were done at room temperature.

The results of this work indicate that curvature plays a significant role in cladding residual stress and that tensile residual stresses as high as the yield stress can be measured in the cladding material. Since the vessel from which the spherical and nozzle corner samples were taken was hydrotested, and the flat plate specimens were taken from specimens used in mechanical fatigue testing, these results suggest that rather high tensile residual stresses can be retained in the cladding material even after some mechanical loading associated with hydrotesting and that higher levels of hydrotest loading would be required to alter the cladding residual stresses.

NOMENCLATURE

FEA Finite Element Analysis

E Young's modulus

ν Poisson's ratio

ID Inside diameter

OD Outside diameter

INTRODUCTION

Residual stress states have become recognized as one of the key ingredients to understanding fatigue, brittle fracture, and stress corrosion cracking mechanisms. Weld deposited austenitic cladding placed on the inside surface of low-alloy ferritic steel is commonly used in pressure vessel construction as an economical way both to protect the contained fluid from contamination by the carbon steel and to protect the carbon steel from attack by the fluid. Unfortunately, the weld deposit process leaves the cladding material in a state of high tensile residual stress that is not reduced significantly by normal post-weld heat-treating processes.

To better understand the magnitude and distribution of the residual stresses in weld deposited cladding, residual stress measurements have been made on a number of different weld clad configurations. The goal of the work is to quantify the residual stress states in the cladding and to determine if thickness and curvature are significant factors in those magnitudes and distributions.

Four different weld configurations were selected: flat pieces, sections from a spherical pressure vessel head, ring-sections from the bore of a nozzle, and sections from a nozzle corner region of a vessel. Cladding thicknesses were between 5 and 9 mm. Total specimen thicknesses including the cladding ranged from 45 mm to 200 mm. Curvature effects were examined by comparing results from flat sections to results from the spherical section, the ring section from a nozzle bore, and nozzle corner sections where local curvatures are significant relative to cladding thicknesses. Two different cladding materials were evaluated

Residual stress results are given graphically for each of the specimens. The principal finding of the study is that 308/309L stainless steel and Alloy 600 weld metal can have similar residual stress states at room temperature and that the thicker the specimen the larger the residual stress. For thick specimens, the residual stress can be near or somewhat larger than the material yield stress while for the thinner sections, the residual stress seems to be at or below the yield stress. Curvature effects were shown to be significant however and, as a general rule, the smaller the radius of curvature relative to the cladding thickness, the larger the residual stress. Mechanical stress relief due to hydrotesting was shown to have less of an effect than curvature on the magnitude of the residual stress in the cladding.

LITERATURE

There is a large literature base describing residual stress states measured and calculated for a variety of weldment configurations. Ferrill, Juhl, and Miller (1966) is typical of papers reporting residual stresses measurements for heavy section weldments using the ASTM E837 hole-drilling technique. As non-linear computational methods have improved, residual stresses have been computed by finite element analysis [FEA] as for example by Friedman (1975), Nickell and Hibbit (1975), and Rybicki, *et al.* (1978).

As technology has improved for both analytical and measurement methods, many papers have been presented on the topic of residual stresses. In fact, over 150 papers on the various methods and results thereof were presented at the Fifth International Conference on Residual Stresses held in Sweden in 1996. At the 1997 ASME Pressure Vessel & Piping Conference, there were several sessions dealing with weld residual stresses and these papers are available in PVP-Vol. 347 edited by Bees (1997).

There have been a number of papers specifically on residual stress measurements in weld deposited austenitic cladding of thick pressure vessels. Bernard, *et al.* (1989) presented measurements of residual stress in thick pressure vessel nozzle cladding and provided a comparison with results of other measurement techniques reported in the literature.

Another class of papers is available where the authors infer the residual stress state from the observed effect on fatigue crack growth behavior. The paper by Cheng and Punch (1997) for stainless steel cladding is an example of such a method. In the paper by Ternon and Faidy (1997) residual stresses in Alloy 600 weld buildup in control rod drive mechanism welds were determined by stress corrosion cracking tests, residual stress measurements, and computations.

These papers all seem to conclude that weld residual stresses depend on weldment geometry, welding process, and weld metal yield stress. The measured residual stress in all of these works is tensile in the cladding and, depending on the process and location, can be as high as the yield stress of the cladding material even after stress relief. The work presented in this paper is intended to add to this information by providing specific weld residual stress measurements for austenitic and Alloy 600 multi-pass weld deposited cladding materials used in typical thick walled pressure vessel construction.

TEST PLAN

Four types of samples were used in this study; specimens cut from flat plates or bars, a specimen cut from a spherical portion of a thick pressure vessel, a ring segment of a nozzle bore, and a transition section of a nozzle-to-shell region including the nozzle corner region. All clad surfaces were machined smooth. Residual stress magnitudes and distributions were measured in the specimens using the layer removal method which is explained later. The effect of thickness and curvature were determined by comparing residual stress magnitudes and distributions from the different specimens. Since the flat samples had been used in fatigue tests and the vessels from which the spherical and nozzle corner sections were taken were hydrotested prior to measuring residual stresses, observations are made regarding the possible effects of mechanical stress relief from prior mechanical loading on the residual stress magnitude.

SPECIMEN DESIGNS

The flat plate specimens were remnants of fatigue crack growth tests. Figures 1a and 1b show the dimensions and orientation of the four flat specimens called Type-1, Type-2, CS-1, and CS-3. The base material of all specimens was low-alloy ferritic steel. The cladding material was overlaid using a standard submerged arc multi-layered process. The specimens were clad and then rough machined to size prior to stress relief at 1150°F for more than two hours per inch of thickness. The specimens were machined to final dimensions and surface conditions after heat treating. The samples were used in fatigue crack growth testing where all applied net stresses were maintained below the yield stress of the base material.

Figure 1a. Flat Plate Type 1 Specimen.

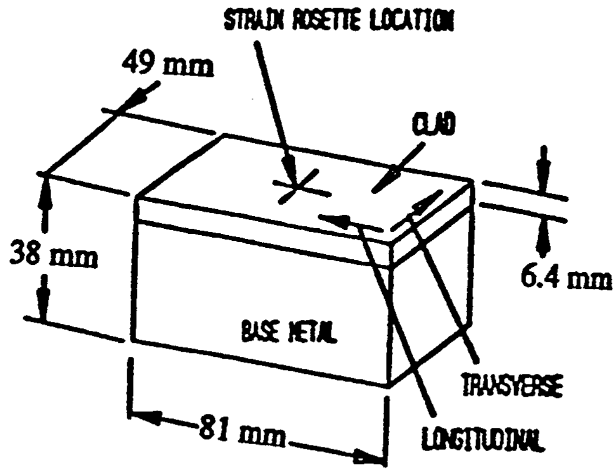

To study the effects of curvature on cladding residual stress, four additional specimens were cut from a low-alloy steel vessel clad with weld-deposited Alloy 600 on the inside surface. The pressure vessel had undergone a stress relief heat-treatment of 1150°F for more than two hours per inch of thickness. One specimen [called SPH] was cut from a spherical section of the lower head of a vessel, one from a ring segment from the bore of a nozzle [called BORE], and two from the nozzle corner regions [called COR-1 and COR-2]. The vessel from which the SPH, COR-1, and COR-2 were taken had been subjected to a typical ASME Boiler & Pressure Vessel Code pre-service hydrostatic test.

Figure 1b. Flat Plate Type 2, CS1, and CS3 Specimens.

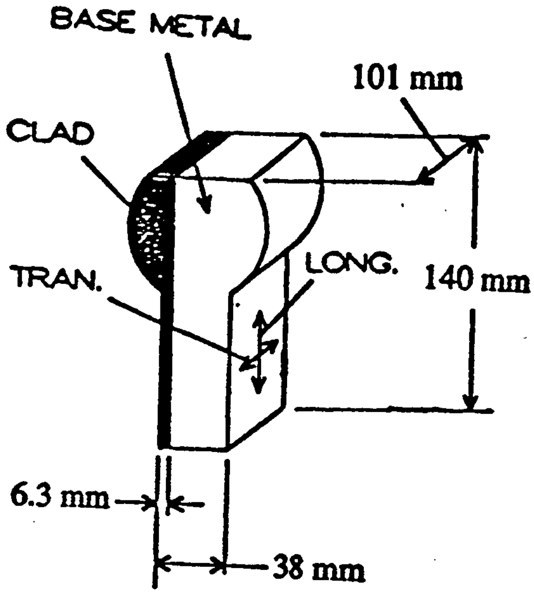

At the location of specimen SPH, shown in Figure 2a, the inside diameter [ID] of the sphere had a radius to thickness ratio (r/t) greater than 6. The clad thickness was 6.4 mm. Specimen BORE, shown in Figure 2b, was obtained from a ring segment with an ID r/t ratio greater than 1 and a cladding thickness of 6.4 mm. COR-1 and COR-2, shown in Figure 2c, were 162 mm thick with COR-1 having a clad thickness of 8.9 mm and COR-2 having a clad thickness of 6.8 mm. COR-1 was taken from the 12 o'clock position of the nozzle (i.e., at a longitudinal intersection of the shell) and the other from the 3 o'clock position (i.e., at the meridional intersection of the shell).

RESIDUAL STRESS EVALUATION METHOD

The method used to evaluate residual stresses is a destructive procedure commonly called the layer removal method. This method involves a series of three cutting and machining operations. Each operation causes a relaxation in the stresses of the remaining piece or pieces. Before any cuts are made, strain gauges are placed at prescribed

Figure 2a. Specimen from Spherical Head.

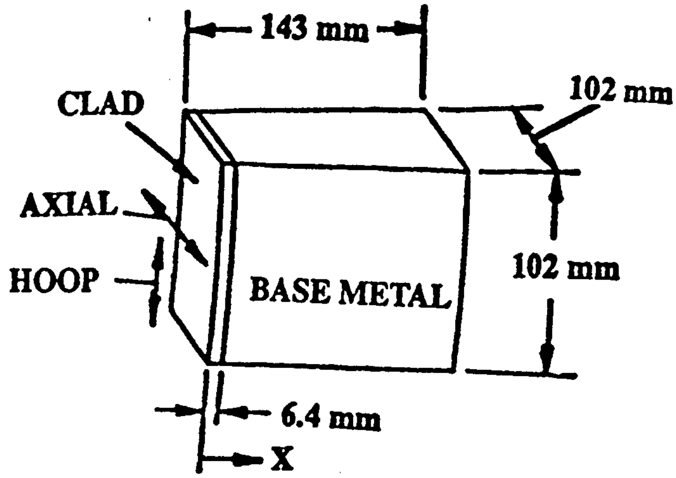

Figure 2b. BORE Specimen.

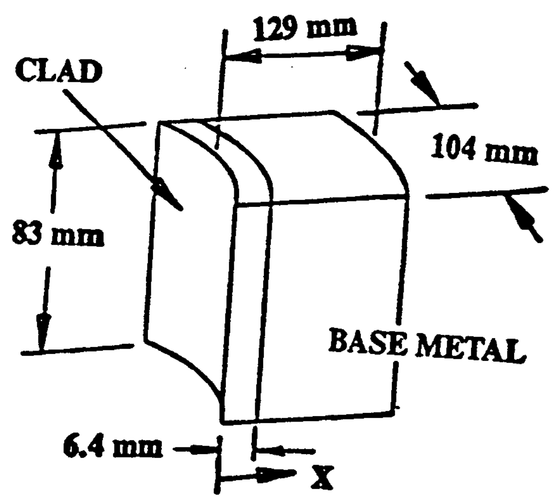

locations on the piece. Changes in strains are recorded following each operation. A back-computation analysis is done to infer the changes in stress in the remaining piece or pieces as well as in the material removed due to machining. The residual stress at any point in the original piece is evaluated by summing the changes in stress at that point due to each machining or cutting operation. The final result is an evaluation of the original residual stress distribution at points through the thickness of the clad and base material. Residual stress results for as many as 27 points through the thickness are provided for each location.

Figure 2c. Nozzle Corner Specimens.

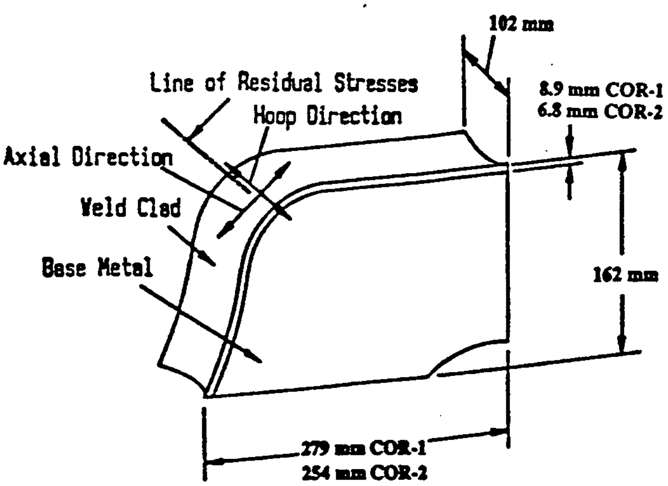

Prior to the layer removal step, two other steps can be used if needed. One step is called *parting-out.* The other step is called *splitting*. The parting-out step is used when the residual stress evaluation piece is part of a very large component, such as a pressure vessel or a large plate. In this case, the residual stress specimen is parted-out of the large component. To evaluate the changes in residual stress due to the parting-out step, strain gauges are placed on the top and bottom surfaces of the piece prior to parting-out as shown in Figure 3. Changes in strain due to parting-out are recorded and input to a back-computation procedure to evaluate the stress changes in the pieces due to the parting-out step. The back-computation procedure is based on principles of mechanics and takes into account the material properties and the geometries of the specimens. Shealy *et al.* (1984) and Shadley (1987) provide information on the back-computation procedures for the parting-out step.

For cases where the parted-out piece is too thick to apply the layer removal method, the splitting step is applied. Figure 4 illustrates the splitting step. The thick piece is split along a plane parallel to the top and bottom surfaces. Strain gauges on the top and bottom surfaces record the changes in strains due to stress relaxation from the splitting step. The changes in stress are calculated using a back-computation procedure for the Consistent Splitting Method described by Rybicki, *et al.* (1983) and Shadley, *et al.* (1985).

Figure 3. Parting-Out of the Specimen.

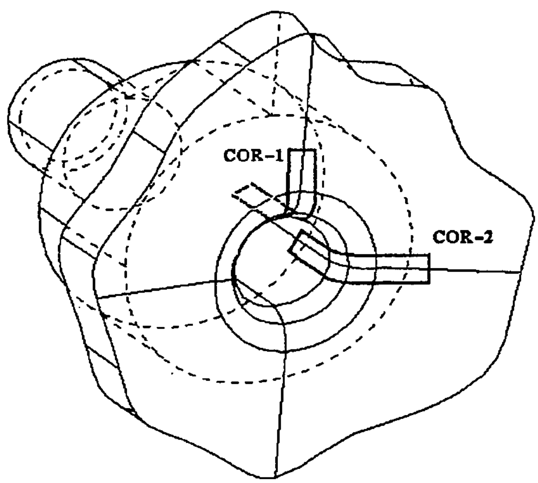

The last machining operation is the layer removal step shown in Figure 5. SAE Handbook (1965) describes the back-computation procedure for the layer removal step. Rybicki et al. (1986) describe how these procedures were applied to a clad plate specimen.

Some improvements to residual stress evaluation laboratory procedures and back-computation procedures were made to account for the different elastic moduli of the clad and base material for the four flat clad specimens evaluated here. The

Figure 4. Splitting of the Specimen.

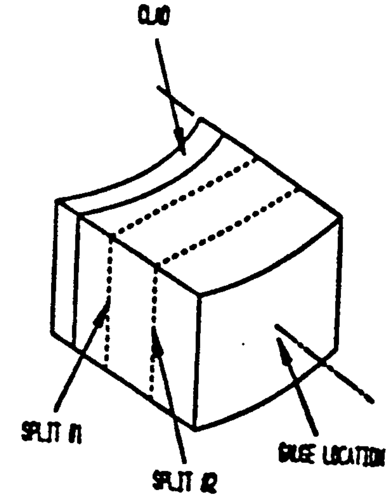

Figure 5. Layering Removal Step.

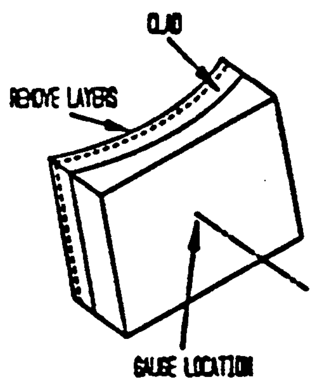

parting-out and consistent splitting back-computation procedures were generalized to allow Young's modulus in the clad to be different from Young's modulus of the base metal. The layer removal back-computation method was modified as described by Greving, Rybicki and Shadley (1994) to account for different moduli in the clad and base material.

The original residual stress distribution is the sum of the changes in stresses due to each step of the residual stress evaluation procedure. The method provides a through-thickness evaluation of the residual stresses in the cladding and base material.

RESULTS: FLAT SPECIMENS

The residual stress evaluation procedure was applied to specimens Type-1, Type-2, CS-1, and CS-3. The parting-out method was needed for specimens Type 2 and CS-3. The splitting step was used on Type 1, Type 2, and CS-1. Layer removal was used on all four specimens.

Young's modulus for the base material that was used was 207 GPa. Young's modulus for the 308/309L stainless steel cladding was 195 GPa and for the Alloy 600 cladding, 163 GPa. Poisson's ratio was assumed to be 0.3 for all materials.

Residual stress results for the four specimens are presented in Figures 6, 7, 8, and 9. Figure 10 shows the results of all the tests averaged for each cladding material type. These results show that there is a much greater specimen to specimen variation in magnitude and distribution than there is for different materials.

Actual yield stress of the cladding material was measured for the stainless steel cladding. The average yield stress of three tests for the 308/309L stainless steel is 307 MPa. Thus, for these tests, the magnitude of the residual stress is about 50% of the as-deposited weld metal yield stress. The yield stress of the as-deposited Alloy 600 weld metal was not measured, but is expected to be somewhat higher than that of the stainless steel.

The residual stress becomes compressive just below the clad-base metal interface reaching a magnitude of about 20% of the expected base metal yield stress. The residual stress decays to near zero at a depth of several clad thicknesses from the clad-base metal interface.

Residual stresses measured by the layer-removal method depend on Poisson's ratio and Young's modulus for the material. To study the effect on accuracy of a 10% error in Young's modulus, the residual stresses were recalculated using a modulus of 207 GPa for both base and cladding material rather than 163 GPa for Alloy 600 and 195 GPa for stainless steel. It turns out that a 10% change in modulus results in about a 10% change in calculated residual stress. Therefore the uncertainty associated with these results is estimated to be somewhat larger than the +/- 5% error associated with typical strain gauge accuracy.

RESULTS: CURVED SPECIMENS

A modulus of 195 GPa and Poisson's ratio of 0.3 was used to obtain all of the results for the vessel specimens. The cladding and base metal were assumed to have the same moduli since the improved technique, previously discussed, had not been incorporated into the test method at the time of this test phase.

The stress distribution obtained for the nozzle BORE specimen is presented in Figure 11. A maximum tensile hoop stress of 315 MPa was obtained in the cladding material. The maximum compressive stresses were between 140 and 180 MPa in magnitude just below the clad-base metal interface. Base metal stresses below a depth of more than about 40 mm are essentially zero. Based on strain gauge information, the stress relieved due to parting-out of the specimen from the nozzle ring was estimated to be about 25 MPa in the axial direction and between 50 to 100 MPa in the hoop direction. Therefore, when added to the sectioning results, an estimate for the peak residual stress in the cladding for the BORE specimen is between 365 and 415 MPa.

Figures 12 and 13 show the residual stress distributions for COR-1 and COR-2. Again the maximum residual stresses for both specimens were in the cladding material. The maximum axial stress in the specimens was approximately 190 MPa while the maximum hoop stress in COR-1 was 170 MPa and 320 MPa in COR-2. Again, the residual stresses changed from tensile in the cladding to compressive in the base metal just under the cladding decaying to near zero several clad thicknesses away from the interface. The residual stresses due to the parting-out step were estimated to be less than 35 MPa.

Residual stress distributions were obtained for two locations on the vessel shell specimen. Figure 14 provides the stress distributions at location #1 and Figure 15 provides the distribution for location #2. A maximum axial stress of about 190 MPa was calculated for the cladding material. The maximum hoop stress for the cladding was calculated to be 255 MPa. The maximum stresses in the base metal, occurring near the clad-base metal interface, were compressive and ranged from 75 MPa to 120 MPa. Base metal stresses attenuated to nearly zero for depths of more than 40 mm below the clad-base metal interface.

CURVATURE EFFECTS

Maximum residual stresses measured in the cladding of the flat specimens were approximately 262 MPa for the 308/309Lstainless cladding and approximately 207 MPa for the Alloy 600 cladding. This compares to stresses between 365 to 415 MPa for the cladding of the BORE specimen. Although it cannot be concluded that these differences are due solely to curvature effects, it is reasonable to conclude that curvature and increased stiffness associated with the bore geometry are important factors in residual stress magnitudes.

MECHANICAL STRESS RELIEF EFFECTS

The flat plate specimens were all taken from remnants of specimens that were originally used in fatigue crack growth tests. These specimens were all cycled many thousands of times to nominal maximum stress levels in the longitudinal direction of about 150 MPa which is below the yield stress of the cladding material. SPH, COR-1, and COR-2 specimens were taken from a vessel that was hydrotested to membrane stress magnitudes roughly equal to the design yield stress of the base material, which is probably above the actual yield stress of the cladding material.

COR-1 was taken at the 12:00 position and COR-2 at the 3:00 position of the nozzle. If the hydrostatic stresses provided a significant stress relief effect, then one would expect the 12:00 position to have lower residual stresses than the 3:00 position and COR-2 since the 12:00 position would have higher tensile hoop stresses than the 3:00 position due to the hydrostatic test. Figure 12 shows that there is little difference in the axial stresses for these two specimens while Figure 13 indicates that COR-1 has a higher value of hoop stress than does COR-2. The residual stress values for the SPH sample shown in Figures 14 and 15 are reasonably similar to those for the flat plate specimens in Figure 8. If mechanical stress relief is present in these specimens, it would be expected to be more evident in the curved specimens than in the flat plate specimens since the curved specimens were loaded to a higher percentage of the yield stress. In addition, if the residual stresses were significantly affected by cyclic loading, it would be expected that the longitudinal residual stress would be lower than the transverse stress which is not the case in the flat specimens.

Although these tests cannot rule out the possibility that prior mechanical loadings of the levels considered here can affect residual stress distributions, the results do suggest that such effects are small.

CONCLUSIONS

Experimental residual stress evaluations were performed on eight clad specimens to determine the through-thickness distribution of residual stress. Measurements were made on flat specimens, specimens taken from the spherical section of a pressure vessel head, and specimens taken from the nozzle bore and nozzle corner region of a pressure vessel. Residual stress evaluations were made using the layer removal method.

The results of this work indicate that curvature can play a significant role in cladding residual stresses and that tensile residual stresses as high as the yield stress can be measured in the cladding material. Since the vessel from which the spherical and nozzle corner samples were taken was hydrotested and the flat plate specimens were taken from specimens used in mechanical fatigue testing, these results suggest that rather high tensile residual stresses can be retained in the cladding material even after some mechanical loading and that these stresses are more affected by local curvature than by local prior mechanical loading history associated with hydrotesting.

ACKNOWLEDGMENTS

This work was performed under a U.S. Department of Energy contract with the Bettis Atomic Power Laboratory, a division of CBS Corporation.

REFERENCES

D.A. Ferrill, P.B. Juhl and D.R. Miller, 1966,"Measurement of Residual Stresses in a Heavy Weldment," Welding Research Supplement, November, pgs. 504s-514s.

Friedman, E., 1975, "Thermomechanical Analysis of the Welding Process Using the Finite Element Method," Journal of Pressure Vessel Technology, Vol. 97, pgs 206-213.

Nickell, R. and H. Hibbit, 1975, "Thermal and Mechanical Analysis of Welded Structures," Nuclear Engineering and Design, No. 32, pgs. 110-120.

Rybicki, E.F., D.W. Schmueser, R.B. Stonesifer, J.J. Groom and H.W. Mishler, 1978, "A Finite Element Model for Residual Stresses and Deflections in Girth-Butt Welded Pipes," Journal of Pressure Vessel Technology, Vol. 100, August, pgs. 256-262.

W.L. Cheng and E. F. Punch, 1997, "Analysis of Fatigue Crack Growth in a Residual Stress Field using Alternating Finite Element Method," PVP-Vol. 354, Current Topics in the Design and Analysis of Pressure Vessels and Piping, ASME PVP Conference 1997.

Bernard, J.L., J. Vagner, A. Pellissier-Tanon, F. Faure, 1992,"Effect of Residual Stresses and Complex Loadings on the Fatigue Behavior of Underclad Cracks," Nuclear Engineering Design, Vol. 133, pgs. 129-138.

Ternon, F., and C. Faidy, 1997, "Residual Stresses and Stress Corrosion Cracking of PWR CRDM Nozzles," Approximate Methods in the Design and Analysis of Pressure Vessels and Piping Components, PVP-Vol. 347, Edited by W. J. Bees, ASME Pressure Vessels and Piping Conference, July, pgs. 193-200.

Shealy, W.S., J.R. Shadley, and E.F. Rybicki, 1984, "An Improved Back-Computation Procedure for the Parting-Out Step of a Destructive Method for Measuring Residual Stresses in Pipes," Strain, Vol. 20, August, pgs. 117-122.

Shadley, J.R. and E.F. Rybicki, 1987, "Application Guidelines for the Parting-Out Step in a Through-Thickness Residual Stress Measurement Procedure," Strain, Vol 23, November, pgs. 157-166.

Rybicki, E.F., J.R. Shadley, and W.S. Shealy, 1983, "A Consistent Splitting Model for Experimental Residual Stress Analysis," Experimental Mechanics, December, pgs. 438-446.

Shadley, J.R. and E.F. Rybicki, 1985, "Experimental Evaluation of Through-Thickness Stresses in a Welded Pipe Using the Consistent Splitting Model," Experimental Mechanics, Vol. 25, No. 2 June, pgs. 115-122.

SAE Information Report, 1965,"Methods of Residual Stress Measurement," SAE J936 Handbook Supplement,J936, December.

Rybicki, E.F., J.R. Shadley, A.S. Sandhu, and R.B. Stonesifer, 1986, "Experimental and Computational Residual Stress Evaluation of a Weld Clad Plate and Machined Test Specimens," J. Engineering Materials and Technology, Vol. 110, October, pgs. 297-304.

Greving, D.J., E.F. Rybicki, and J.R. Shadley, 1994, "Residual Stress Evaluations of Thermal Spray Coatings by a Modified Layer Removal Method," The J. of Thermal Spray Tech., Vol. 3 No. 4, December, pgs. 379-388.

Figure 6. Residual Stress Distribution for Sample TYPE-1; A302B Base metal; 308/309L Cladding.

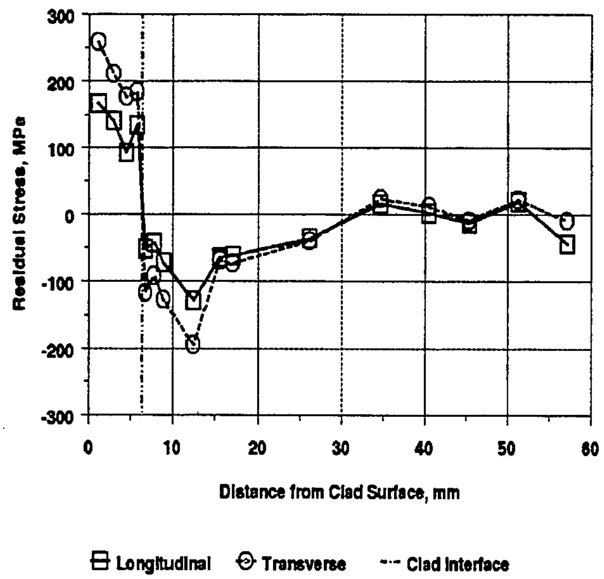

Figure 7. Residual Stress Distribution for Sample TYPE-2; A302B Base metal; 308/309L Cladding.

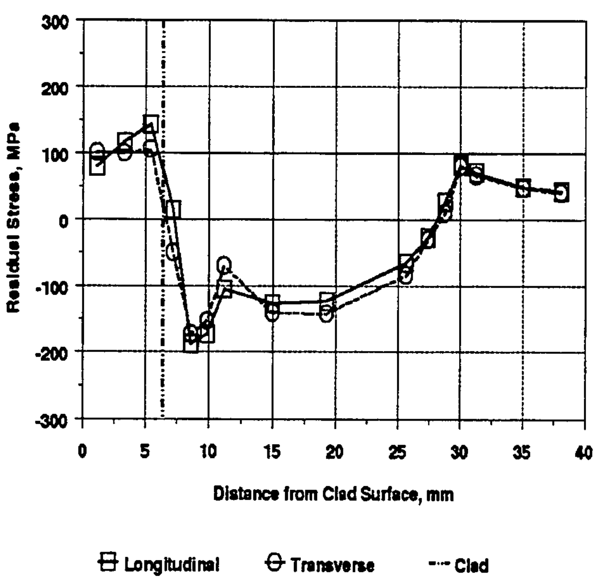

Figure 8. Residual Stress Distribution for Sample CS-1; A508 Cl. 2 Base metal; Alloy 600 Cladding.

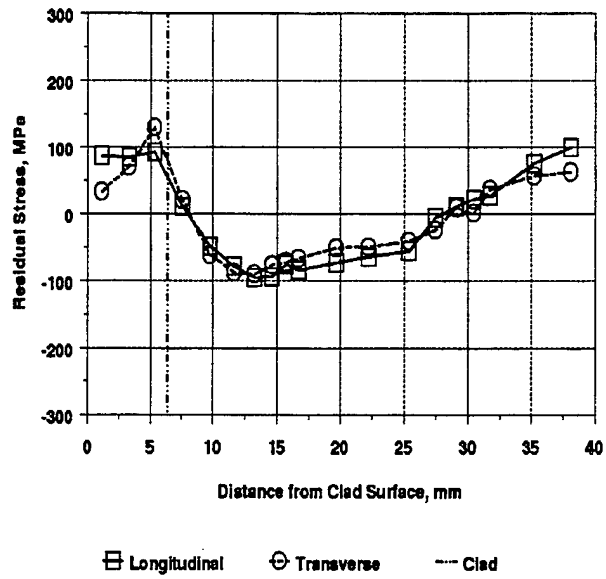

Figure 9. Residual Stress Distribution for Sample CS-3; A508 Cl. 2 Base metal; Alloy 600 Cladding.

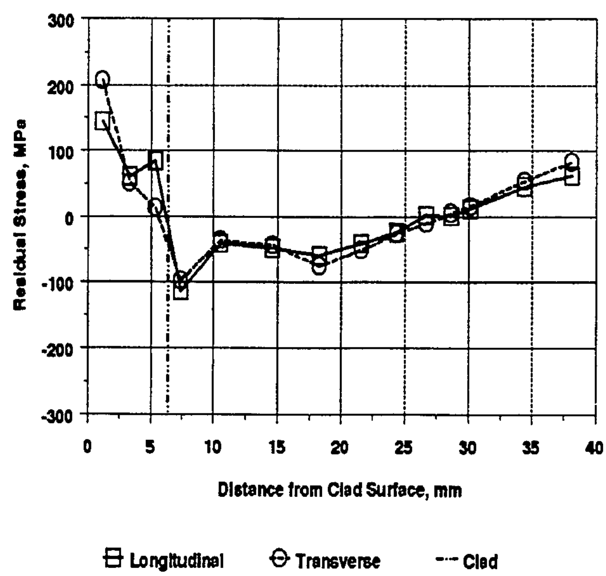

Figure 10. Comparison of Average Residual Stress for Each Cladding Material.

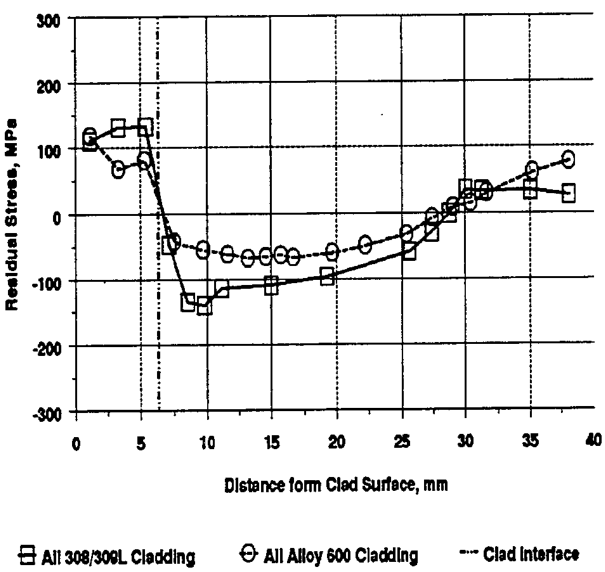

Figure 11. Residual Stress Distribution for Clad Nozzle BORE Sample.

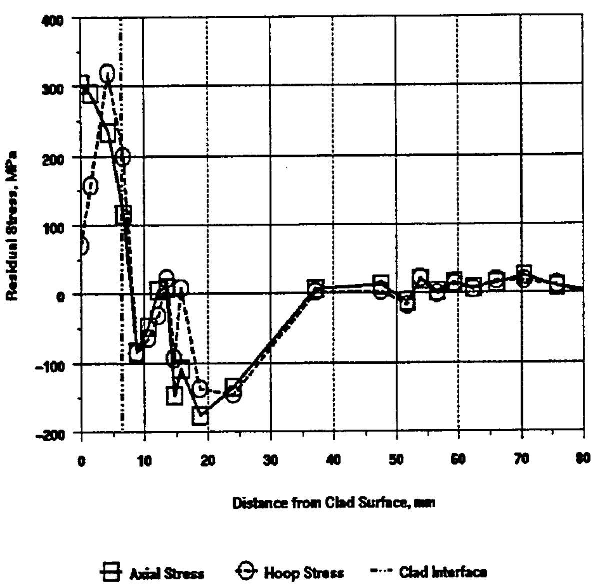

Figure 12. Comparison of Axial Residual Stress Distribution in Clad Nozzle Corner.

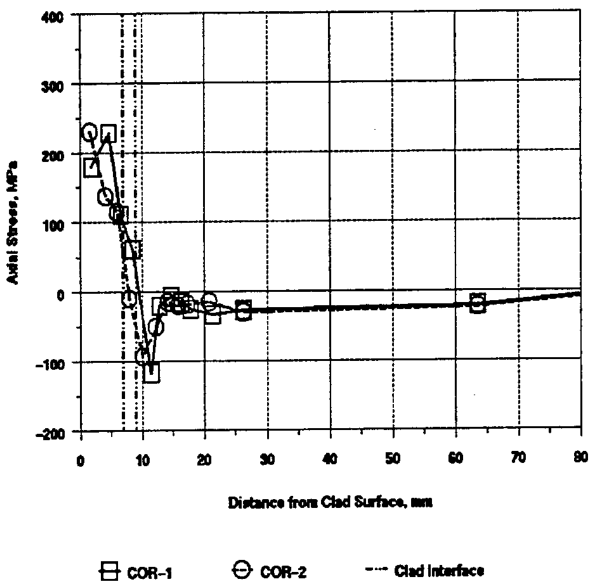

Figure 13. Comparison of Hoop Residual Stress Distribution in Clad Nozzle Corner.

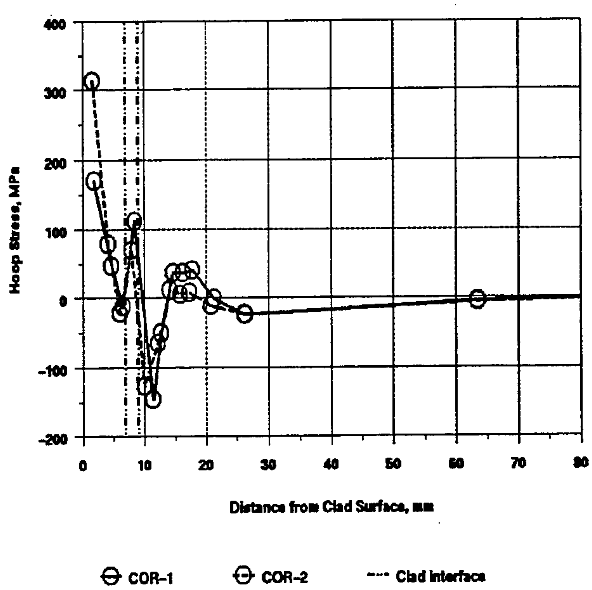

Figure 14. Residual Stress Distribution in Clad Vessel Shell: Location #1.

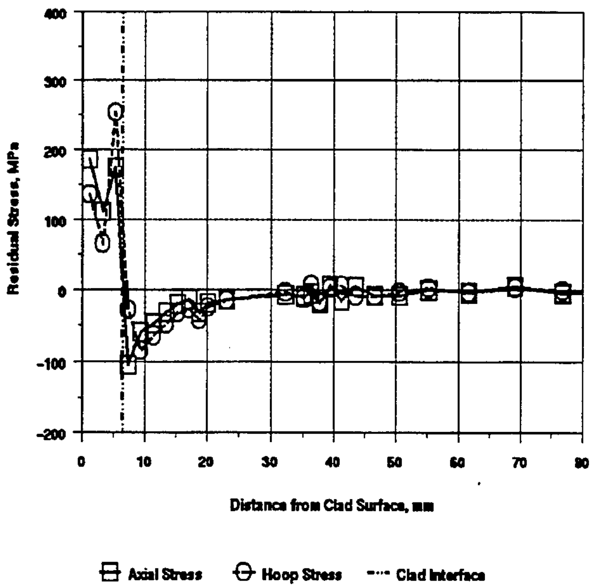

Figure 15. Residual Stress Distribution in Clad Vessel Shell: Location #2.

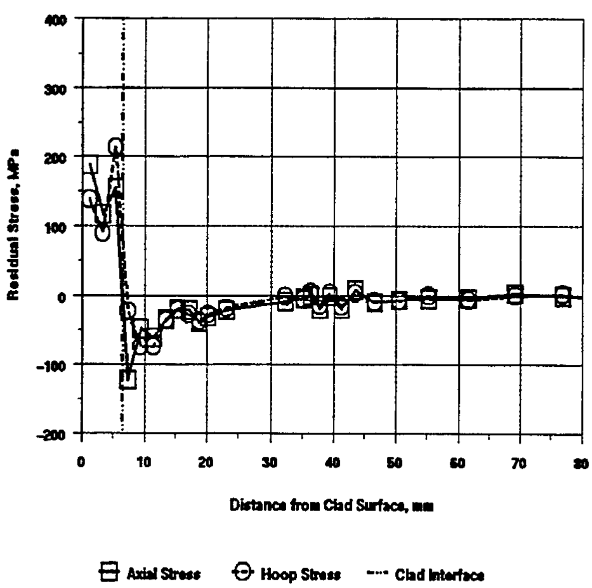

Report Number (14) WAPD-T--3181
CONF-980708--

Publ. Date (11) 199807
Sponsor Code (18) DOE/NE, XF
UC Category (19) UC-504, DOE/ER

no 1332.15 in folder

DOE